JOURNAL OF CRITICAL REVIEWS

ISSN- 2394-5125 VOL 7, ISSUE 04, 2020

PLUG-AND-PLAY COMPLIANT CONTROL HYBRID SYSTEM FOR MICRO-GRID

K. Rakesh Kumar[1], Dr. A. Srujana[2]

[1]PG scholar, Department of Electrical and Electronics Engineering Vidya Jyothi Institute of Technology, Aziz Nagar Gate, C.B. Post, Hyderabad-75

[2]Professor, Department of Electrical and Electronics Engineering Vidya Jyothi Institute of Technology Aziz Nagar Gate, C.B. Post, Hyderabad-75

Abstract: This paper proposes a microgrid control system that is compatible with plug-and-play, consisting of PV, Wind and fuel cell sources. The control with power sharing capabilities of inverter-based microgrids is a difficult task because of the unique nature of microgrid stability. Wind and fuel cells are linked to inverters for load demand synchronization in the proposed PV source system. In particular, if the ratio x/ r is near unity and the lines are short, drop-controlled microgrids will become unstable. Digital impedance is considered to be one of the promising instruments to avoid this form of instability, which enables a large range of drops to efficiently share power between the inverters. But the correct size of the virtual impedance is still an open problem for a specific microgrid configuration. To improve the reliability of droop modes, the size of virtual impedance in a plug-and - play system is proposed. Both numerical simulations using the MATLAB / Simulink verify the operation of the virtual impedance with the suggested stability enhancement method.
Keywords: PV, wind, fuel-cell, microgrid mode, plug-and-play.

I. INTRODUCTION

Micro automated operating systems – micro-grid systems (MG) – made energy efficient manuscript feasible by creating cost-effective battery storage with high bandwidth inverter interface; obtained the 1 June 2018 Energy Supply; revised on 21November 2018; approved on 9January 2019. Date of publication: 24 January 2019; 18 June 2019. This research has been financed in part by the MUSES project, in part by the University of Khalifa, MIT, Cambridge, MA, Relation from the United-States 02 / MI / MIT / CP/11/07633 / GEN and part of the next generation of the SKOLTECH-MIS program. Don't remember that. Don't remember that. TPWRS-00838-- The Maschinist Technology Institute of Massachusetts (e-Mail:,pohsu0113@gmail.com) was in HUANG at TPWRS-00838-- HUANG. P. Vorobev has been working with the Mechanical Engineering Department of the Technical Institute of Massachusetts, Cambridge, US MA 02139. Now she is to the Skolkovo Science and Technology Center in Moscow 121205, Russia (Email:,p.vorobev@skoltech.ru). M. Al Hosani was at the Electrical and Computer Engineering Department, Khalifa University, Abu Dhabi 54224 UAE. He is now at the Abu Dhabi Distribution Center in Abu Dhabi, UAE. J. MA 02139 United States (e-mail:, kirtley@mit.edu) L. Kirtley is working at the Electric and Computing Department of Massachusetts Institute of Technology, Cambridge. K. Turitsyn has collaborated with MA 02139 (email: turitsyn@gmail.com) from the Department of Mechanical Engineering, Massechusetts Technology College in Cambridge. At http:/ieeexplorer.ieee.org you can find online color versions of one and more of the statistics. 10.1109 / TPWRS.2019.2895081 Uncontrollable renewable sources of virtual object recognition without grid connections to support network activity. Therefore, controlling inverter or inverter systems gains significant interest, thus posing specific challenges compared to traditional power systems. Various control systems are commonly preferred by droop-base control, since they provide many benefits such as contact-free power sharing, high expansion, high plug-and - play efficiency and a similar power control to synchronous computer systems[1]–[4]. The control systems provide the same advantages. The drop control is focused solely on local behavior that involve the requisite electricity distribution between multiple mode-forming inverters to ensure the proper power sharing and durability of the system. The close relation of active power to frequency and reactive power to voltage enables these systems to be implemented with the high X / R ratios in modern power systems. It has also proposed a strategy for AC-related converters [5], or for IBMGs [1], [3], [4]. However, because of much

ISSN- 2394-5125 VOL 7, ISSUE 04, 2020

less X / R unit ratios for IBMGs, the coupling between real power and frequency is distorted because studies indicate small-signal stability regions for the potential increases of microgrid droppings in comparison with conventional grids[6]. In most experiments, this issue was discussed on a reasonably realistic assumption that the dynamics of the electromagnetic networks – a typical approximation of conventional power systems – were not taken into consideration and backed by a distinct distinction in time between network and power control modes[7]–[10]. However, in light of their short time scope,[1][12], an experimental and comprehensive simulations in IBMGs have demonstrated a much less than quasi-stationary approximation in the real stability area . In fact, this reflects the value of electromagnetic transients. A recent study showed the influence on the dynamics of slow power controller modes of these rapid degrees of freedom[12]. The relatively low impedance of the network (which results in strong interconnections among the various inverters) is one of the key reasons for instability of a standard IBMG which is fully consistent with the experimental findings found in[13]. There is therefore a strong reason for the virtual stabilization impedance of IBMGs. The theory that naturally strong connections in IBMGs are abolished has led to numerous studies to improve the effective impedance of the line by physical or virtual methods[10] [14] – [19] before an understanding of the value of electromagnetic transients is understood. In particular, emulating inductive dynamics by means of a digital controller saves massive, costly inducers through increased precision and stability in power sharing. The control is generally carried out by the modulation of voltage settings with a calculated current output in order to imitate an impedance 's dynamic behavior, which results in a virtual impedance linked to the internal tension source of a terminal[14]. However, the right option for literature instability is not known as virtual impedance dimension. Current methods usually are based either on complex models with linearized self-values[13] or on highly simplistic models such as oscillators from Kuramoto[7]. It is incredibly unintuitive and time consuming to work on complicated high-order models, while simpler models tend not to predict specific stability limits. Thus it is a practical requirement to build a guideline for control engineering that preserves simplicity and faithfulness. We note that in microgrids there are different forms of instability, but the basic requirement is limited signaling stability that is essential for all microgrid forms and configurations. This paper focuses on the derivation of small-signal stability rules and methods to improve the stability of micro-grids. The problem is studied first and reduced-order models are applied to provide physical insight into the root of drop insecurity. Then, Lyapunov 's feature candidates are proposed to achieve a succinct stability criterion based on the model of a reduced order of a single two-bus example and on a wider network. Finally, Plug and Play (PnP) has compatible design rules for selecting virtual impedances and linkages, including a set of arbitrary ratings. The solution proposed allows for the rapid and effective incorporation of inverters only through the implementation of certain local legislation in microgrid systems. A variety of models ranging from small to complex are then tested for the system. The key contribution is summed up in this document:

1) In order to achieve the desired stability area, simple and accurate virtual impedance size parameters are derived and evaluated.

2) The modular integration of droop-controlled inverters into microgrids is expected to comply with the plug-and -play rules (PnP).

3) A detailed review of the proposed approach in order to show its feasibility and efficacy in particular models

II. EXISITNG SYSTEM

The simulation models used in MATLAB / Simulink in this segment to test the validity of the suggested solution with detailed application of control loops. The Linmod and trim functions are used to remove linearized transformation matrices and their own values for computing the Simulink model's stability field. Additionally, the constant power load is often regarded with the use of industrial PFC power supplies as well as voltage change transformers, Since the power and voltage of the foundation are decreased for logical testing. Both simulation and implementation have the same base impedance, so that the pu system parameters are the same. See the machine configuration Fig.1

ISSN- 2394-5125 VOL 7, ISSUE 04, 2020

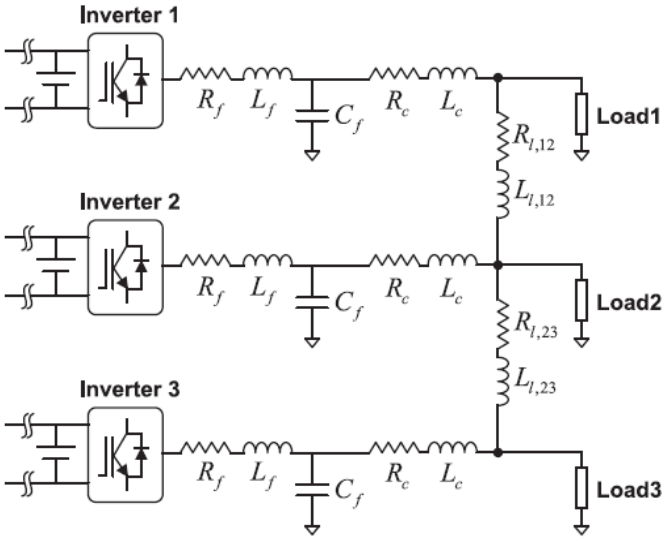

Fig.1 Three-inverter test system

TABLE I: PARAMETERS OF THREE INVERTER TEST SYSTEM

Parameter	Description	Value
V_b	Base voltage (simulation)	381 V
S_b	Base power (simulation)	5 kVA
V_b	Base voltage (prototype)	71 V
S_b	Base power (prototype)	174 VA
Z_b	Base impedance	29 Ω
ω_0	Nominal frequency	$2\pi\times50$ rad/s
w_c	Frequency filter constant	$2\pi\times5$ rad/s
f_{sw}	Switching frequency	10 kHz
σ_i	Voltage feed-forward gain	1
σ_v	Current feed-forward gain	0.5
L_c	Coupling inductance	0.35 mH
R_c	Coupling resistance	80 mΩ
L_f	Filter inductance	1 mH
C_f	Filter capacitance	30 µF
R_{vd}	Virtual damping resistance	5 ohm
C_{vd}	Virtual damping capacitance	0.25 mF
k_{pc}, k_{ic}	Current loop PI gains	8, 18 000
L_l	Line inductance	$0.26\,\text{mH km}^{-1}$
R_l	Line resistance	$165\,\text{m}\Omega\,\text{km}^{-1}$
l_{12}	Line length (Bus 1 to 2)	0.6 km
l_{23}	Line length (Bus 2 to 3)	3.25 km

III. PROPOSED SYSTEM

You can see the system configuration at Fig. 2.The proposed system consists of three PV-, WIND-connected inverters, fuel cell and resistor, inductor, condenser (Rf, Lf, Cf) filters, connecting resistor Rc and Lc, line resistor and condenser arrangement as shown in fig2. The use of commercial PFC power supply in conjunction with the voltage transformer, which decreases both base and voltage power, also indicates constant energy load.

ISSN- 2394-5125 VOL 7, ISSUE 04, 2020

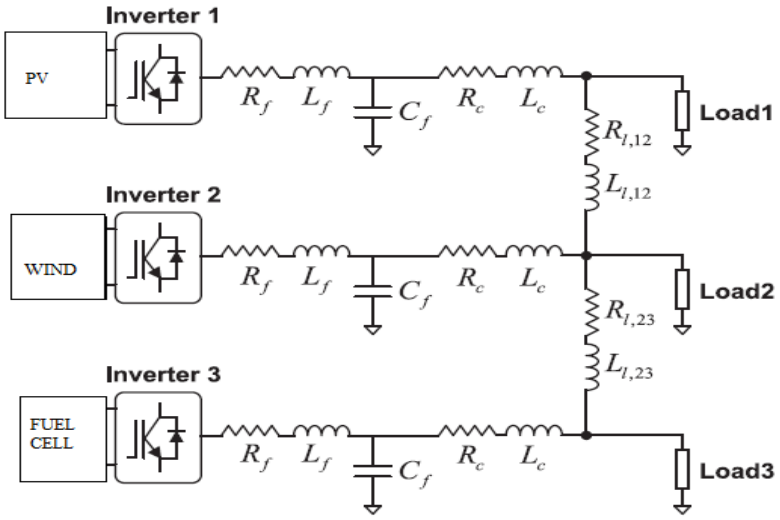

Fig 2. Proposed three-inverter test system

IV. DROOP INSTABILITY OF INVERTER-BASED MICROGRID

An external (power) drop controller that provides references to internal control loops regulate inverter voltage and frequency, is required for a standard drop-controlled inverter system. Fig.3[1] shows the main structure of the inverter. The measured signals are the indicated internal reference structure for the internal control circuit; a powerful current control circuit regulates a high bandwidth filter current;

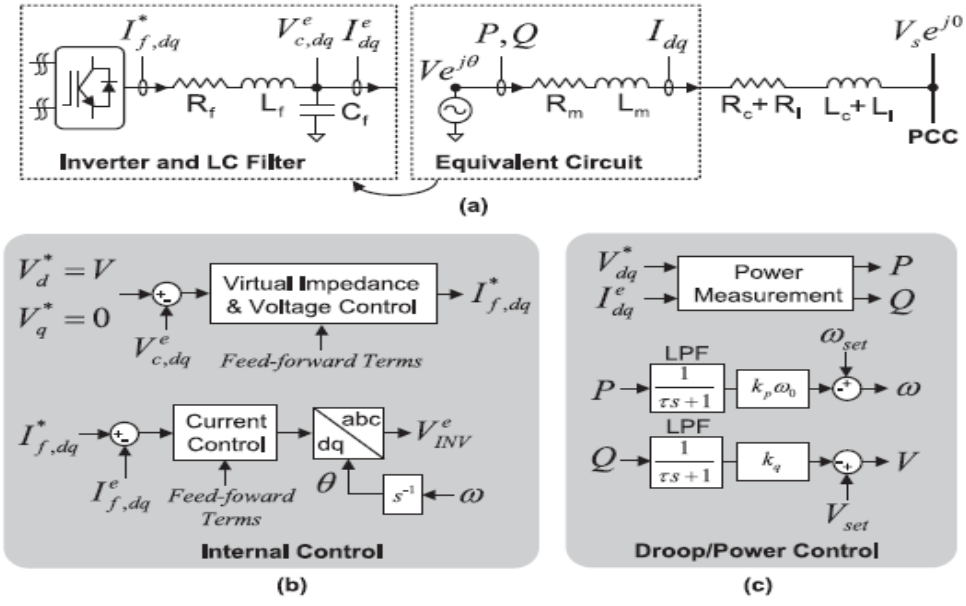

Fig..3 (a) System arrangement of an inverter associated to the PCC. (b) Internal control. (c) Drop (power) control

ISSN- 2394-5125 VOL 7, ISSUE 04, 2020

Various modifications in the form of voltage control have already been proposed. Digital emulation of impedance has proven efficient for several purposes, including improvement of stability, harmonic sharing, reactive power sharing, etc. Apart from presupposing the emulation of virtual impedances for checking stability for power sharing, due to the slower time scale of the power control, an internal control will be enough to be seen as an impedance of the series (Rm, Lm shown in Fig.3(a). The high drop power control increases have been reported in low-frequency drop modes[1],[13],[22]. For a typical microwave, the maximum allowed active power fall ratio could be considerably reduced. A direct study of the importance of detailed models in the high-order system was conducted in order to explore rich and complicated stability conditions, in which little understanding has been given to the causes of instability. The writers in a previous piece[12] revealed a different understanding of physical stability. This section will start by briefly presenting the basic framework, which will allow the development of concise stability criteria for droop managed IBMGs in the following section.

V. MODELING OF THE SIMPLE TWO-BUS SYSTEM

In the event that the Common Coupling Point (CCP) is a rigid voltage source as indicated in Fig.1(a), the following ODEs may characterize the Electromagnetic Model as a drop-operated inverter as the steep Bus Reference Frame:

$$\dot{\theta} = \omega - \omega_0 \tag{1}$$

$$\tau\dot{\omega} = \omega_{set} - \omega - k_p\omega_0 P \tag{2}$$

$$\tau\dot{V} = V_{set} - V - k_q Q \tag{3}$$

$$L\dot{I}_d = V\cos\theta - V_s - RI_d + \omega_0 LI_q \tag{4}$$

$$L\dot{I}_q = V\sin\theta - RI_q - \omega_0 LI_d \tag{5}$$

Whenever the internal tension source's relative angle to the bus is 0, the bus' rigid tension frequency is 0, the control filters' frequency is μ= c; the frequency and voltage are −set and the Vset are the respectively frequency and voltage points; μp and kq are the real frequency and tension respectively of the internal tension source; p and Q are the active and reactive control of the internal tension source; kp and kq are¨. Also, it is still not easy to analyze this relatively simple 5th order model So for certain functions, the left sides of 4 and 5 are set to null. This results in the use of various approaches to evaluate the decreased order model similar to the oscillator system of Kuramoto. The typical reason for this measurement is that the network dynamics (L / R) time constant is typically reduced significantly in several milliseconds in relation to the power control constant (approx.). 30 m. However, for a stability evaluation of IBMGs[11][22], this method of approximation was shown to be inadequate, although the time scale of the electro-magnetic phenomenon is small. A more accurate reduction model was proposed for this function[12]:

$$\lambda_p\tau\ddot{\vartheta} + (\lambda_p - B')\dot{\vartheta} + B\vartheta + G\rho - G'\dot{\rho} = 0 \tag{6a}$$

$$(\lambda_q\tau - B')\dot{\rho} + (\lambda_q + B)\rho - G\vartheta + G'\dot{\vartheta} = 0 \tag{6b}$$

where $\vartheta \triangleq \delta\theta$, $\rho \triangleq \delta V$, $\lambda_p = (k_p\omega_0)^{-1}$, $\lambda_q = k_q^{-1}$, and:

$$G = \frac{R}{R^2 + X^2},\ B = \frac{X}{R^2 + X^2}, \tag{7a}$$

$$G' = \frac{L(R^2 - X^2)}{(R^2 + X^2)^2},\ B' = \frac{2LXR}{(R^2 + X^2)^2}. \tag{7b}$$

ISSN- 2394-5125 VOL 7, ISSUE 04, 2020

Model (6) helps us to see in instability the function of electro-magnetic transients – the term B reduces efficient damping of the device. A basic qualitative stability evaluation can be inferred as −p −b > 0, i.e. a coefficient sign in front of the −function. We get a harsher expression in the sub-section below. It is worth noting that even highly charges lead to very small variations in angles and voltage fluctuations in the inverter-focused microgrid as seen from [11], [12], [23], due to the low network impedance values per device. One of the implications is that the reliability of the small signals is basically independent of the operating stage, Which corresponds entirely to the results of the experiment[13]. With this assumption-actually equations (6) arising from conditions of small angle variations or voltage fluctuations in the inverter operating points, complex equations and stabilization conditions have been greatly simplified. This can be used only in such highly stressful situations as these emergency microgrid systems (line currents several hundred or more) are true at any normal operating point. In considering these unrelated states, it is an independent issue that goes beyond the scope of this research (not just from the perspective of low signal stability).

VI. STABILITY ASSESSMENT

Simple formula (6) can be used to evaluate stability by certain expert techniques. The system consistency test is especially useful for the definition of a true Lyapunov function V(x)>0. The accuracy of the method can be checked if the time derivative is negative. V [x] lower than 0. Although it is usually a non-trivial problem to produce an effective candidate function for the arbitrary systems, quadratic candidates for Lyapunov give satisfactory results for linear systems. We begin by multiplying (6a) by (c) in order to receive Lyapunov candidates:

$$\begin{aligned}&\frac{d}{dt}\left\{\frac{\lambda_p(\tau\dot{\vartheta}+\vartheta)^2}{2}+\frac{(c\tau\bar{B}-B')\vartheta^2}{2}+\frac{(c-1)\tau^2\lambda_p\dot{\vartheta}^2}{2}\right\}\\&+\tau((c-1)\lambda_p-cB')\dot{\vartheta}^2+B\vartheta^2+G\vartheta\rho-G'\vartheta\dot{\rho}\\&+c\tau G\dot{\vartheta}\rho-c\tau G'\dot{\vartheta}\dot{\rho}=0\end{aligned}\tag{8}$$

Relationships like 2 pages = d / dt(derive) have been used here to move those terms under a complete derivative symbol. Multiply (6b) by (cμ μl +) to achieve the same: Multiply (cć)

$$\begin{aligned}&\frac{d}{dt}\left\{\frac{((c+1)\tau\lambda_q+c\tau B-B')\rho^2}{2}+(c\tau G+G')\vartheta\rho\right\}\\&+(\lambda_q+B)\rho^2+c(\tau^2\lambda_q-\tau B')\dot{\rho}^2-G\vartheta\rho\\&-G'\vartheta\dot{\rho}-c\tau G\dot{\vartheta}\rho-2c\tau G\vartheta\dot{\rho}+c\tau G'\dot{\vartheta}\dot{\rho}=0.\end{aligned}\tag{9}$$

Adding (8) and (9) together yields:

$$\frac{1}{2}\frac{d\mathcal{V}}{dt}=-\mathcal{Y}\tag{10}$$

Where the lyapunov function candidate V is quadratic form V = yT p y with y = [ć) where the lyapunv functions as candidate V are quadratic form V = yT p y with y:

$$P=\begin{bmatrix}\lambda_p & 0 & 0 & 0\\ 0 & (c-1)\tau^2\lambda_p & 0 & 0\\ 0 & 0 & c\tau B & c\tau G\\ 0 & 0 & c\tau G & (c+1)\tau\lambda_q+c\tau B\end{bmatrix}\tag{11}$$

For the decay rate $\mathcal{Y}$, likewise, we have the following quadratic form $\mathcal{Y}=z^TQz$, where $z=[\vartheta,\tau\dot{\varrho},\tau\dot{\vartheta},\varrho]^T$ and matrix Q:

$$Q=\begin{bmatrix}B & -cG & 0 & 0\\ -cG & c\lambda_q-\frac{c}{\tau}B' & 0 & 0\\ 0 & 0 & \frac{c-1}{\tau}\lambda_p-\frac{c}{\tau}B' & 0\\ 0 & 0 & 0 & \lambda_q+B\end{bmatrix}\tag{12}$$

ISSN- 2394-5125 VOL 7, ISSUE 04, 2020

In order to be stable, both Lyapunov function V and the decreasing rate Y have to be positive in the system. similar to the positive definitivity of the matrices of P and Q. (11) and (12); Simple equations finish under P 0 conditions (we presume c > 1), respectively:

$$\lambda_p > 0 \qquad (13a)$$

$$\frac{c+1}{c}\lambda_q + B - GB^{-1}G > 0 \qquad (13b)$$

Likewise, matrix Q is positive definite if:

$$\lambda_p > \frac{c}{c-1}B' \qquad (14a)$$

$$\lambda_q - B'/\tau - cGB^{-1}G > 0 \qquad (14b)$$

$$\lambda_q + B > 0 \qquad (14c)$$

If one assumes that λp> 0 and λq> 0 Eqs The Circumstances. (13a), and (14c) still catch up. The state in (14b) is potentially more strict than (13b) as c > 1, B > 0 and B > 0. Thus, if two conditions are met, namely eqs, positive interpretation of both P and Q is guaranteed. By (14a) and (14b). Suppose

$$\lambda_p > \frac{c}{c-1}B', \qquad \lambda_q > cGB^{-1}G, \qquad (15)$$

The coefficients kp and kq for frequency and tension decrease are:

$$k_p < \frac{c-1}{c\omega_0 B'}, \qquad k_q < \frac{B}{cG^2}, \qquad (16)$$

The effect of B on the stability of the system is especially obvious from these equations and, in particular, B is significantly hit in the active frequency mode. Equations (16) represent adequate stability for each value of constant c on the kp and kq levels corresponding to a rectangular area (see Fig. 4.2). The following simplified stability criterion is obtained by combining all those regions-ranging from 1 to infinity-:

$$\mathrm{B}\ \omega 0\mathrm{kp} + \Gamma\mathrm{kq} < 1 \qquad (17)$$

Where Γ = G2 /B.

The above stabilization conditions are described by Fig. Fig. 4.2 where the predicted stability fields are compared to the frequency and voltage drop coefficients of different c values in the equations (16) and the predicted average stability area of (17). Equations (1) to (5) and (6) are often suggested by their limits of stability through direct numerical analysis. We also include the stability region which is anticipated for the feasibility of the proposed approximations in the detailed high order model (see section IV, for some of the model's parameters). Although the kq projections in all cases are very conservative, True reactive power gains typically do not impact on the extended stability spectrum.

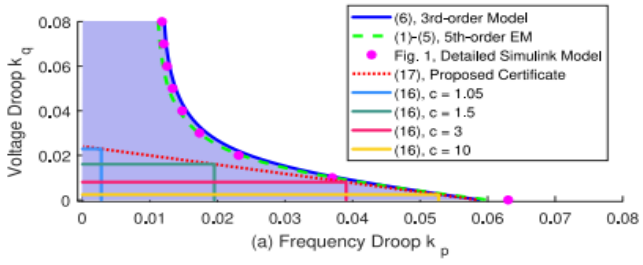

ISSN- 2394-5125 VOL 7, ISSUE 04, 2020

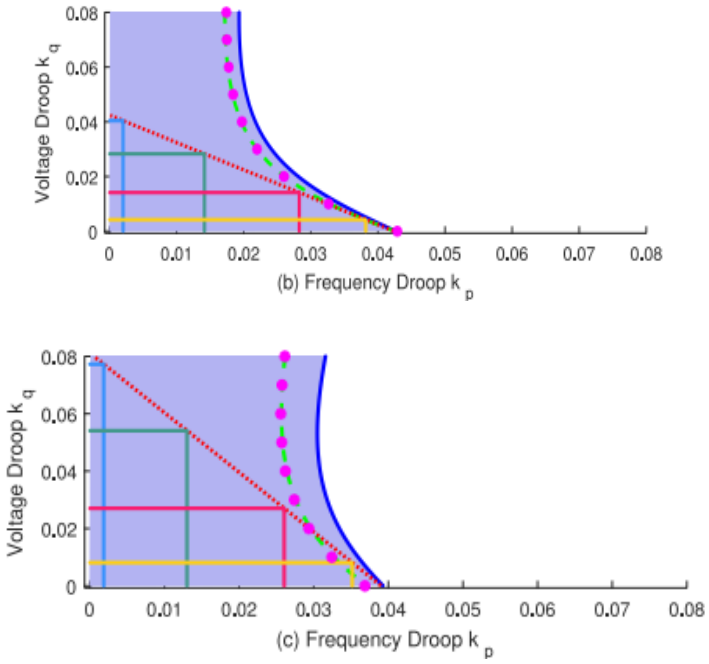

Fig. 4 The two-bus system's limited signal stability regions are based on various models regarding voltage and frequency drop gains (|Z| = 3%): (a) X/R = 0.667; (b) X/R = 1; (c) X/R = 1.5.

This suffers from unsymmetric network setups, so droop losses are less efficient in allowing for given sharing ratios). Beyond the suggested stability credential, the reduced-order configuration can also be seen to continue to perform well while the X / R is near unit. So for practical reasons we'll add the statement in the later section. In the end, the analysis of (7) and (17) indicates that changes in PCC impedance increase the permissible area of drops. In particular, B- is the most binding concept which can result in very high frequency drop gains constraints for the normal setting of microgrids.

VII. SIMULATION RESULTS

A. EXISITNG RESULTS

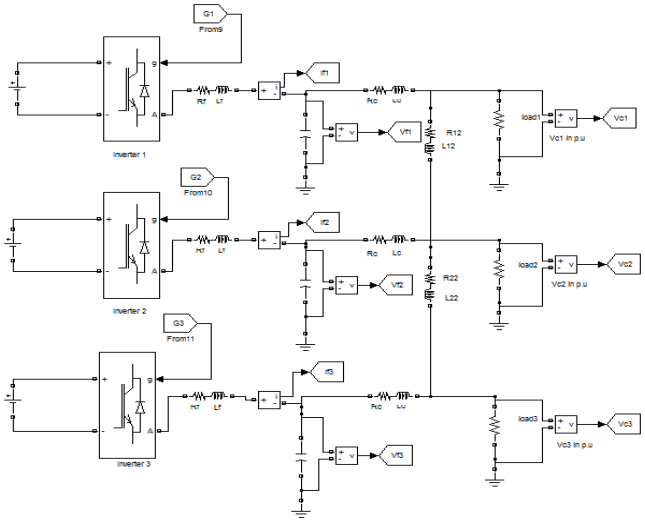

Fig 5. MATLAB/SIMULINK circuit of existing system

ISSN- 2394-5125 VOL 7, ISSUE 04, 2020

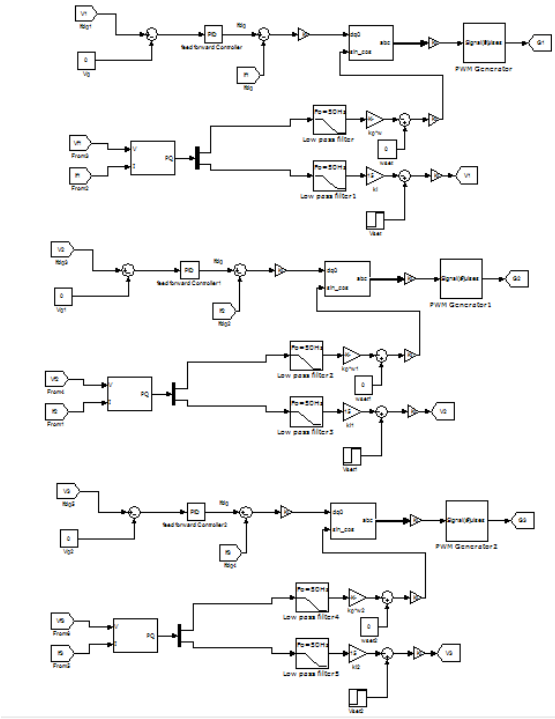

Fig 6. controller subsystem

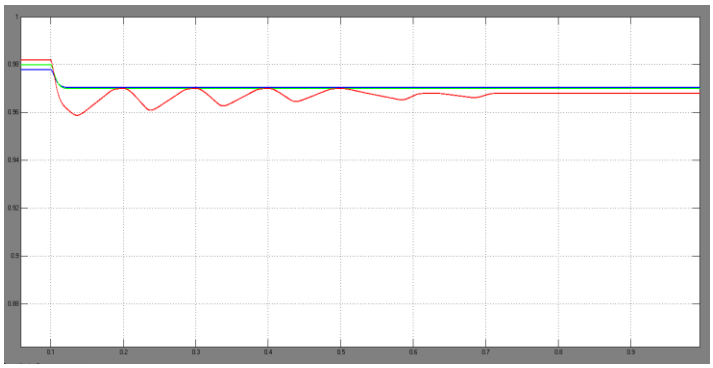

(a)

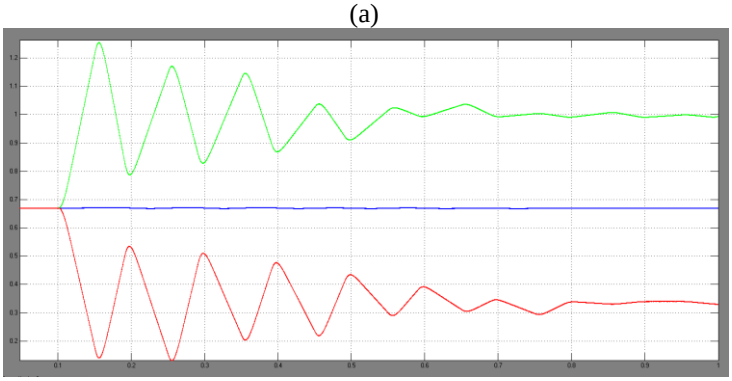

ISSN- 2394-5125 VOL 7, ISSUE 04, 2020

(b)

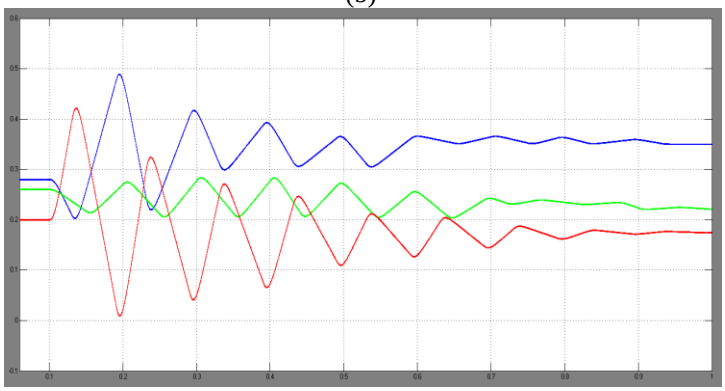

(c)

Fig7. Time-domain results for a step change of sharing ratios, *si* , form1 : 1 : 1 to 1 : 0.67 : 0.33: *kp* ,*i* = *kq* ,*i* = 2/*si*%; *Xmc,i* = *Rmc,i* = 2/*si*%; (a) output voltages (*Vc*); (b) filtered active power; (c) filtered reactive powers of inverter1, inverter2, and inverter3

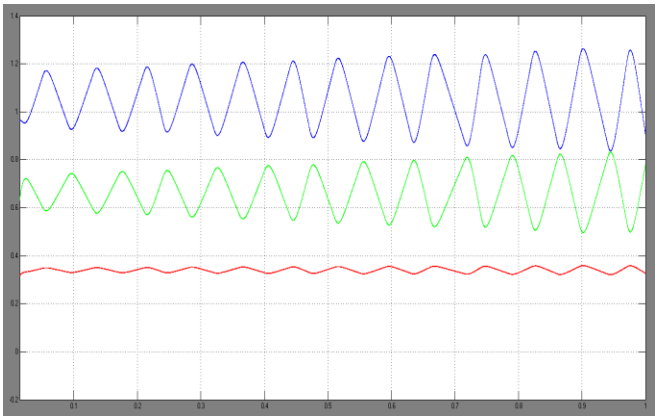

(a)

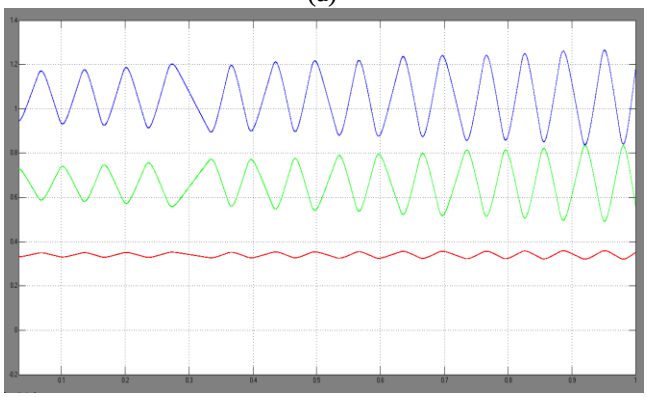

(b)

Fig8. Droop oscillations beyond critically stable conditions: sharing ratios 1 : 0.67 : 0.33,*Xmc,i* = *Rmc,i* = 2/*si* %; (a) *kp* ,*i* =2.8/*si* %, *kq* ,*i* = 2/*si*%; (b) *kp* ,*i* = 4.3/*si*%, *kq* ,*i* = 0/*si*%. For inverter1, inverter2, and inverter3

ISSN- 2394-5125 VOL 7, ISSUE 04, 2020

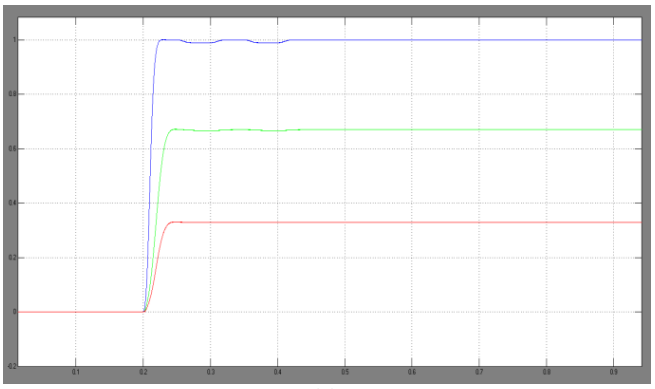

(a)

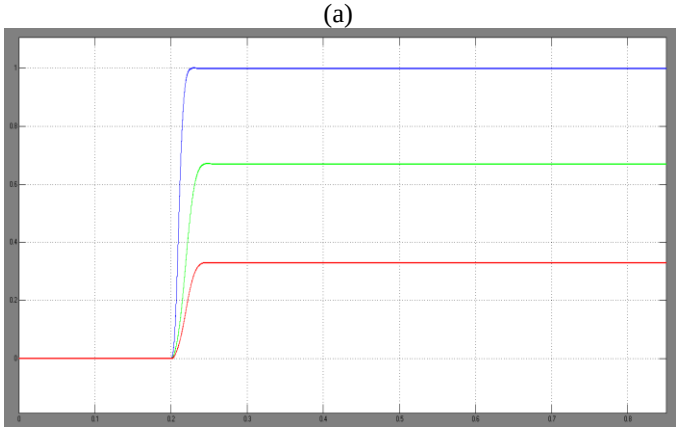

(b)

Fig9. Dynamic responses of filtered active power during load stepping: sharing ratios 1 : 0.67 : 0.33, *kp* ,*i* = 2/*si* %, *kq* ,*i* = 2/*si*%; (a) *Xmc,i* = *Rmc,i* = 2/*si*% (b) *Xmc,i* = *Rmc,i* = 5/*si* %.For inverter1, inverter2, and inverter3

EXTENSION RESULTS

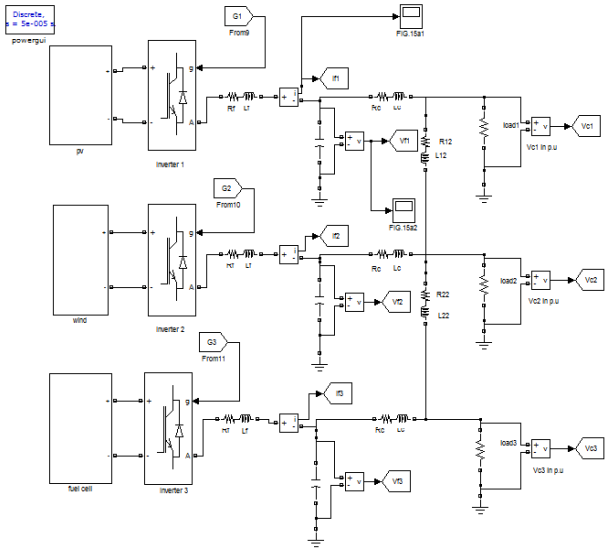

Fig 10 MATLAB/SIMULINK circuit of Proposed system

ISSN- 2394-5125 VOL 7, ISSUE 04, 2020

The time domain research is conducted on the basis of both measurement and simulation, in addition to validating the stabilisation regions. We 're using a fairly high drop gain in particular to show that the solution to virtual impedance will effectively dampen droop oscillations. After a phase change in 1 : 1 : 1 to 1 : 0.67 : 0.33 sharing ratios, the complex responses of the system are seen in Fig.11, in the same loading condition as the previous article.
In this situation all losses and virtual impediments change step by step from 0.1s-kp, I = kq, I = 2 / si% and Xmc, I = Rmc, I = 2 / si%. Active and reactive power distribution varies according to reciprocal ratios; oscillation damping due to the conservative nature of the proposed PnP rules; decrease in tension and frequency due to an overall increased virtual impedance and decreased gains;;

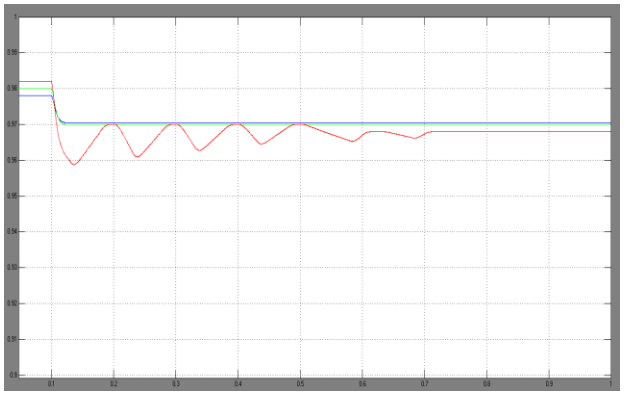

(a)

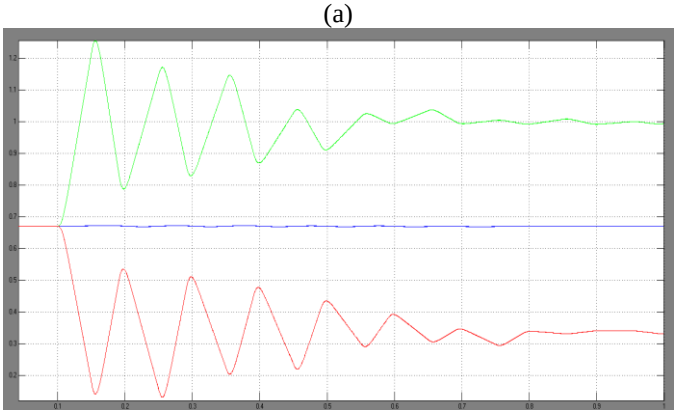

(b)

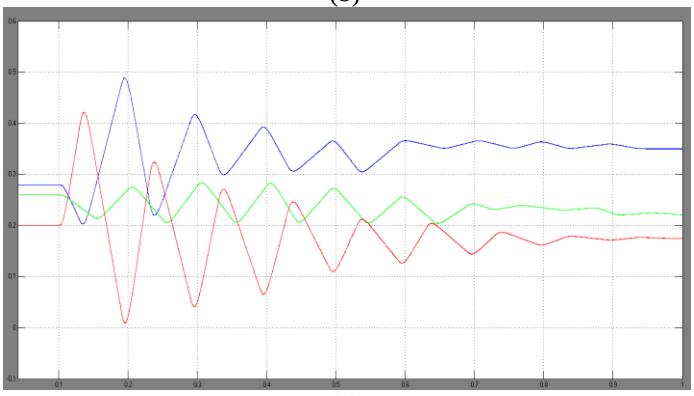

(c)

Fig. 11 Time-domain results for a shared relationship change step, if, form1 : 1 : 1 to 1 : 0.67 : 0.33: *kp ,i = kq ,i = 2/si%; Xmc,i = Rmc,i = 2/si%*; (a) output voltages (*Vc*); (b) filtered active power; (c) filtered reactive powers of inverter1, inverter2, and inverter3

ISSN- 2394-5125 VOL 7, ISSUE 04, 2020

Fig.12 shows the reported oscillations in two highly stable operating conditions. Higher rates of oscillation can be seen as resulting in small losses of active power droop. Furthermore, as contrasted with inverter 3, the critical interaction between inverters 1 and 2 leads to a superior magnitude of oscillation in between.

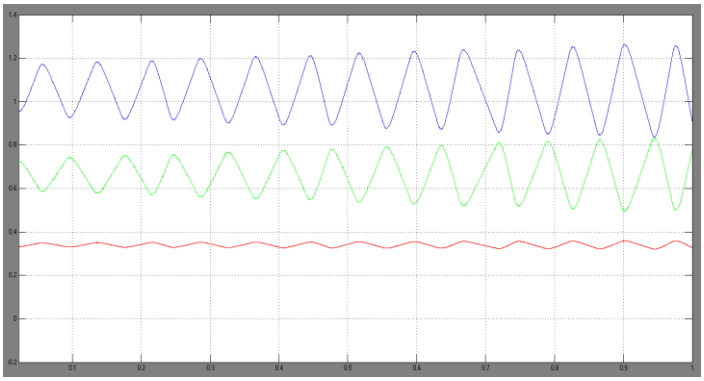

(a)

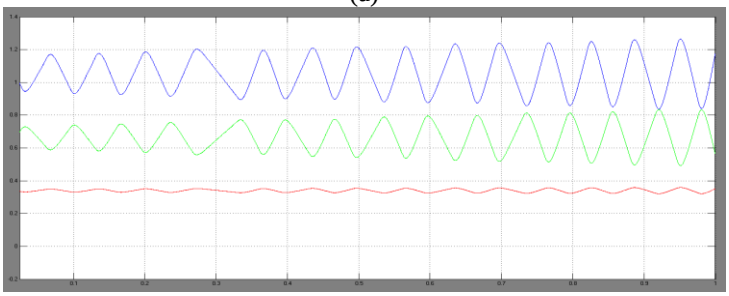

(b)

Fig 12 Fall over critically stable conditions: ratios of sharing 1 : 0.67 : 0.33,*Xmc,i* = *Rmc,i* = 2/*si* %; (a) *kp* ,*i* =2.8/*si* %, *kq* ,*i* = 2/*si*%; (b) *kp* ,*i* = 4.3/*si*%, *kq* ,*i* = 0/*si*%. For inverter1, inverter2, and inverter3

Fig.13 displays the voltage responses dependent on various values of controlled impedances for a sudden resistive load walking of 2 pu. In general, the transient voltage drops in simulation are about 0.88 to 0.94 pu for a few hundred microseconds and are not prone to the regulated impedance, as they are primarily influenced by internal power, network characteristics;

And forms and places to fill. In a steady state, the voltage variations can be observed in proportion to the degree of the control impedance as predicted.

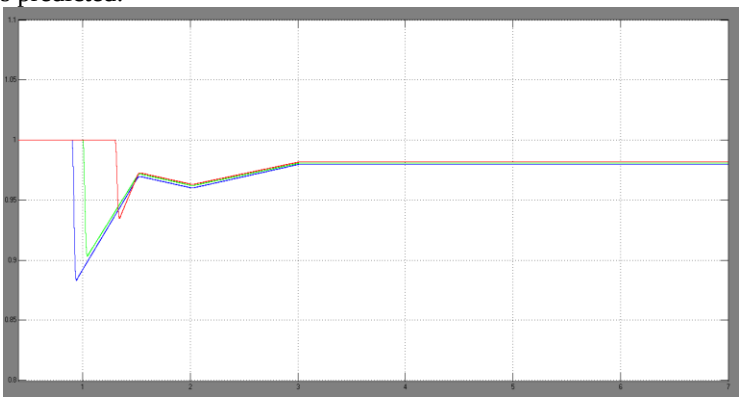

(a)

ISSN- 2394-5125 VOL 7, ISSUE 04, 2020

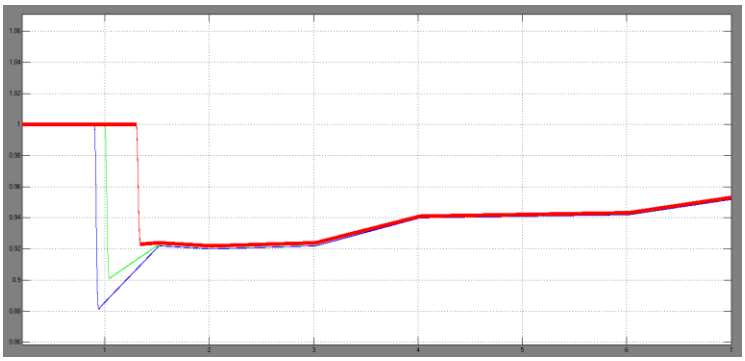

(b)

Fig. 13. Dynamic responses of output voltages (Vc) during load stepping: sharing ratios 1 : 0.67 : 0.33, kp ,i = 2/si %, kq ,i = 2/si%; (a) Xmc,i = Rmc,i = 2/si% (b) Xmc,i = Rmc,i = 5/si%.

The active-power responses filtered on the same dataset are seen in Figure 14. Due to broad time fluctuations in filtering, the responses are nearly similar, regardless of the differences in voltage response.

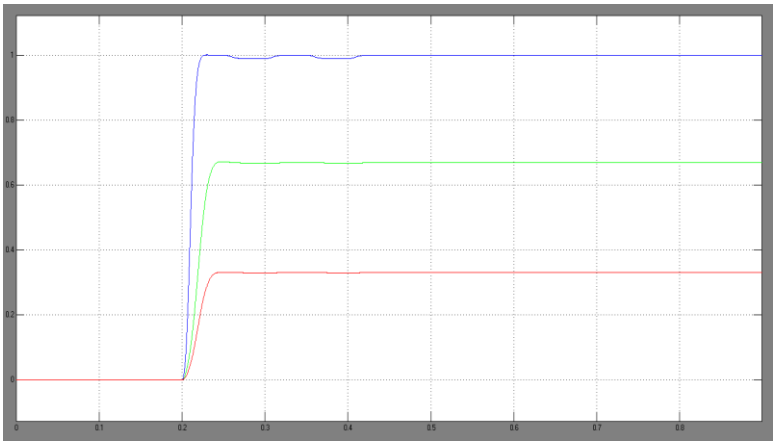

(a)

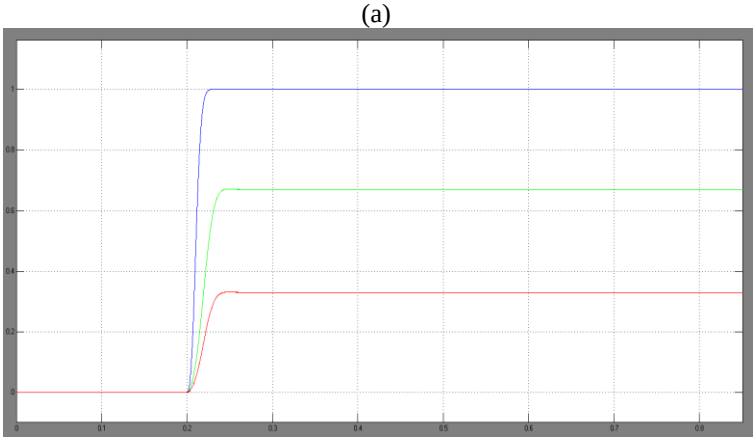

(b)

Fig.14 Dynamic responses of filtered active power during load stepping: sharing ratios 1 : 0.67 : 0.33, *kp ,i* = 2/*si* %, *kq ,i* = 2/*si*%; (a) *Xmc,i* = *Rmc,i* = 2/*si*% (b) *Xmc,i* = *Rmc,i* = 5/*si* %.For inverter1, inverter2, and inverter3

ISSN- 2394-5125 VOL 7, ISSUE 04, 2020

CONCLUSION

Complex microgrid architecture with high impedance values per unit line, and where the X / R ratio in drop-controlled mode is almost unitary leads to instability. The stability of electromagnetic line is primarily caused by delays, With a modest network size in particular. In the form of a simulated impedance emulated by inverter controls, we examined in detail a potential solution to this problem. The simulated impedance scaling is obtained and examined to ensure reliability in sharing operations with a drop-in alternative. It has been shown that IBMG reliability requirements have been tested in a variety of local conditions to improve virtual impedance, allowing efficient monitoring and control of play and spatial decision-making. The inverters are also attached to the PV, wind and fuel cells for stable operation.

REFERENCES

[1] N. Pogaku, M. Prodanovic, and T. C. Green, "Modeling, analysis and ´ testing of autonomous operation of an inverter-based microgrid," IEEE Trans. Power Electron., vol. 22, no. 2, pp. 613–625, Mar. 2007.
[2] D. E. Olivares et al., "Trends in microgrid control," IEEE Trans. Smart Grid, vol. 5, no. 4, pp. 1905–1919, Jul. 2014.
[3] J. M. Guerrero, J. C. Vasquez, J. Matas, L. G. De Vicuna, and M. Castilla, ˜ "Hierarchical control of droop-controlled ac and dc microgridsa general approach toward standardization," IEEE Trans. Ind. Electron., vol. 58, no. 1, pp. 158–172, Jan. 2011.
[4] E. Planas, A. Gil-de Muro, J. Andreu, I. Kortabarria, and I. M. de Alegr´ıa, "General aspects, hierarchical controls and droop methods in microgrids: A review," Renew. Sustain. Energy Rev., vol. 17, pp. 147–159, 2013.
[5] M. C. Chandorkar, D. M. Divan, and R. Adapa, "Control of parallel connected inverters in standalone ac supply systems," IEEE Trans. Ind. Appl., vol. 29, no. 1, pp. 136–143, Jan./Feb. 1993.
[6] N. Hatziargyriou, Microgrids: Architectures and Control. Hoboken, NJ, USA: Wiley, 2013. [7] J. W. Simpson-Porco, F. Dorfler, and F. Bullo, "Droop-controlled inverters ¨ are kuramoto oscillators," IFAC Proc. Volumes, vol. 45, no. 26, pp. 264– 269, 2012.
[8] Y. Zhang and L. Xie, "Online dynamic security assessment of microgrid interconnections in smart distribution systems," IEEE Trans. Power Syst., vol. 30, no. 6, pp. 3246–3254, Nov. 2015.
[9] E. Coelho, P. Cortizo, and P. Garcia, "Small-signal stability for parallelconnected inverters in stand-alone ac supply systems," IEEE Trans. Ind. Appl., vol. 38, no. 2, pp. 533–542, Mar./Apr. 2002.
[10] J. M. Guerrero, L. G. De Vicuna, J. Matas, M. Castilla, and J. Miret, "A wireless controller to enhance dynamic performance of parallel inverters in distributed generation systems," IEEE Trans. Power Electron., vol. 19, no. 5, pp. 1205–1213, Sep. 2004.
[11] V. Mariani, F. Vasca, J. Vasquez, and J. Guerrero, "Model order reductions ´ for stability analysis of islanded microgrids with droop control," IEEE Trans. Ind. Electron., vol. 62, no. 7, pp. 4344–4354, Jul. 2015.
[12] P. Vorobev, P.-H. Huang, M. Al Hosani, J. L. Kirtley, and K. Turitsyn, "High-fidelity model order reduction for microgrids stability assessment," IEEE Trans. Power Syst., vol. 33, no. 1, pp. 874–887, Jan. 2018.
[13] E. Barklund, N. Pogaku, M. Prodanovic, C. Hernandez-Aramburoand, and T. C. Green, "Energy management in autonomous microgrid using stability-constrained droop control of inverters," IEEE Trans. Power Electron., vol. 23, no. 5, pp. 2346–2352, Sep. 2008.
[14] J. He and Y. W. Li, "Analysis, design, and implementation of virtual impedance for power electronics interfaced distributed generation," IEEE Trans. Ind. Appl., vol. 47, no. 6, pp. 2525–2538, Nov. 2011.
[15] Y. W. Li and C. N. Kao, "An accurate power control strategy for powerelectroncis-interfaced distributed generation units operating in a lowvoltagemultibusmicrogrid," IEEE Trans. Power Electron., vol. 24, no. 12, pp. 2977–2988, Dec. 2009.
[16] J. M. Guerrero, L. G. de Vicuna, J. Matas, M. Castilla, and J. Miret, "Output impedance design of parallel-connected UPS inverters with wireless loadsharing control," IEEE Trans. Ind. Electron., vol. 52, no. 4, pp. 1126–1135, Aug. 2005.
[17] J. He, Y. W. Li, J. M. Guerrero, F. Blaabjerg, and J. C. Vasquez, "An islanding microgrid power sharing approach using enhanced virtual impedance control scheme," IEEE Trans. Power Electron., vol. 28, no. 11, pp. 5272– 5282, Nov. 2013.
[18] H. Tian, Y. W. Li, and P. Wand, "Hybrid ac/dc system harmonics control through grid interfacing converters with low switching frequency," IEEE Trans. Ind. Electron., vol. 65, no. 3, pp. 2256–2267, Mar. 2018.

ISSN- 2394-5125 VOL 7, ISSUE 04, 2020

[19] W. Yao, M. Chen, J. Matas, J. M. Guerrero, and Z.-M. Qian, "Design and analysis of the droop control method for parallel inverters considering the impact of the complex impedance on the power sharing," IEEE Trans. Ind. Electron., vol. 58, no. 2, pp. 576–588, Feb. 2011.
[20] X. Wang, Y. W. Li, F. Blaabjerg, and P. C. Loh, "Virtual-impedance-based control for voltage-source and current-source converters," IEEE Trans. Power Electron., vol. 30, no. 12, pp. 7019–7037, Dec. 2015.
[21] J. Kim, J. M. Guerrero, P. Rodriguez, R. Teodorescu, and K. Nam, "Mode adaptive droop control with virtual output impedances for an inverterbased flexible ac microgrid," IEEE Trans. Power Electron., vol. 26, no. 3, pp. 689–701, Mar. 2011.

AUTHOR'S PROFILE

K. Rakesh kumar was born in Ramagundam, Telangana, in 1995. He received Bachelor of Engineering degree in Electrical and Electronics Engineering in the year 2017 from Mother Therssa Engineering College,Peddapally,Telangana state. Present he is pursuing M.Techin the Department of Electrical & Electronics Engineeringin Vidhya Jyothi Institute of Technology, Aziz Nagar, Hyderabad-75,Telangana state, India.His area of interest isControl of Electrical Drives, Power Quality, FACTS, and renewable energy system.Email id: rakeshkaleru212@gmail.com

Dr.A.Srujana, completed her Bachelor's Degree from Kakatiya Institute of Technology &Science, Warangal, and M.tech in Power electronics from JNTU, Hyderabad. She has worked at various capacities in prominent Engineering colleges as Principal, Professor and HOD. She has Guided fifteen M.tech projects & is guiding three Ph.D students. She has about 21 years of Experience in Academics. Her areas of Interest are Power Electronics, FACTS, HVD and Power Systems. Currently she is working as Professor & HOD in the Department of Electrical and Electronics Engineering at Vidya Jyothi Institute of Technology, Aziz Nagar Gate, C.B. Post, Hyderabad-75.